Desalination and Water Treatment
www.deswater.com

doi: 10.5004/dwt.2018.21841

104 (2018) 304–314
February

Kinetic study of food dyes removal from aqueous solutions by solar heterogeneous photocatalysis with artificial neural networks and phytotoxicity assessment

W.J. Do Nascimento Júnior[a], O.R.S. da Rocha[b,*], Renato F. Dantas[c], J.P. da Silva[b], A.A. Barbosa[b]

[a]*Chemical Engineering Faculty, State University of Campinas (UNICAMP), Albert Einstein Av. 500, 13083-852, Campinas, Brazil, email: welenilton@gmail.com*
[b]*Department of Chemical Engineering, Federal University of Pernambuco (UFPE), Prof. Arthur de Sá av., Cidade Universitária, Recife, Brazil, Tel. +55(81)21267322; emails: otidene@hotmail.com (O.R.S. da Rocha), josivan_silva@hotmail.com (J.P. da Silva); adabarbosa@hotmail.com (A.A. Barbosa)*
[c]*School of Technology, State University of Campinas (UNICAMP), Paschoal Marmo 1888, 13484-332, Limeira, Brazil, email: renatofalcaod@hotmail.com*

Received 27 July 2017; Accepted 22 December 2017

ABSTRACT

Effluent treatment for food industry wastewater is a subject of growing concern among the scientific community. Synthetic dyes are a major case and their presence can disturb aquatic environments and introduce highly toxic potentials to the ecosystem, even at low concentrations. In this study, the chemical kinetics of a degradation process was studied for the treatment of a Tartrazine (E102) and Brilliant Blue (E133) solution by different methods. First, the efficiency of eight advanced oxidative processes systems was investigated in their treatment. The most efficient result was obtained in a UV-solar/H_2O_2/TiO_2 system, which reached a degradation percentage of 99.36% in 180 min. Second, a 2^3 factorial planning was used to enhance quantitative degradation in this system and a similar result (99.21%) was reached in 90 min with the optimal conditions. The kinetics of this experiment was fitted in a pseudo-first-order model and the rate constant (k) estimated as 0.0541 min^{-1}. An artificial neural network was developed for the experiment to describe the degradation behaviour over time with a minimum error. Chemical oxygen demand and conductivity were estimated in order to assure the environmental quality of the samples. A *Lactuca sativa* bioassay revealed an upturn in LC_{50}, the concentration to inhibit 50% of the organism growth, from 39.31% (v/v) to 87.73% (v/v). The result indicates a highly favourable reduction in acute phytotoxicity, that coupled with quantitative efficiency, makes the proposed use of solar light as radiation source and improvements in water quality parameters a suitable tool for large-scale synthetic dye treatment.

Keywords: Tartrazine; Brilliant Blue; Advanced oxidation processes; Heterogeneous photocatalysis; Artificial neural networks

1. Introduction

Dyes are largely applied in the food industry in order to improve the visual quality of the products, which is an important factor for consumers [1]. Synthetic dyes are favoured due to their high stability to light, oxygen, heat and pH variation and also providing homogeneous colouration

* Corresponding author.

1944-3994/1944-3986 © 2018 Desalination Publications. All rights reserved.

when applied [2]. The concern relies on the fact that around 10%–20% of these substances are released during the manufacturing process and are easily incorporated into water bodies [3,4], compromising watercolour, light penetration and oxygen dissolution, consequently affecting the maintenance of aquatic life [1,5]. Some even represent a threat to human health [6] suspected of presenting carcinogenic, neurotoxic and genotoxic potential [1,5,7]. Many countries have already banned the use of some synthetic food dyes [7,8] such as Brilliant Blue (BB) and Tartrazine (TT), which have been prohibited in many European countries and regulated in many others around the world [9].

TT or E102 (Fig. 1(a)) is an azo anionic dye highly soluble in water used to apply a lemon-yellow colour to cakes, jams, bubble gums, cookies, ice cream, sauces and sweets in general and in the soft drink industries [10–13]. TT is pointed out to be the most allergenic azo dye to human [2,11] and the acceptable daily intake for TT is 7.5 mg per kg of body weight [13]. BB or E133 (Fig. 1(b)) is a weak organic acid, highly ionic from the triphenyl methane group [14]. For many years, BB has been applied to jams, syrups, dairy and bakery products, sports drinks and it is also largely used in the formulation of drugs [15,16]. The mixture of TT and BB can produce different shades of green for drinks, candies and chewing gums [17].

Food dyes are high absorbents of light in the visible region of spectra, which makes them suitable to be detected by UV–visible spectroscopy, a simple and low-cost technique [7,17]. TT presents maximum absorbance peak at 425 nm while BB at 630 nm [6,17], thus there is no spectral overlay. However, Antakli et al. [17] noted an interference in the absorbance peaks of TT and BB when mixed in solution, explaining a slight difference between the referenced values of wavelength and the wavelength at the highest absorbance peaks.

Due to complexity, high molecular weight and chemical stability, the removal of these molecules represents a challenge which requires alternative treatment technologies [11,18]. Synthetic dyes removal has been explored by different technologies, such as adsorption, chemical coagulation, membrane separation, electrochemical degradation and advanced oxidative processes (AOPs) [18,19]. AOPs are chemical oxidation processes based on free radicals generation, mainly hydroxyl (•OH) and peroxyl (•OOR) radicals, that can attack non-selective organic molecules oxidising them to CO_2, water and other by-products. The most studied systems include potent oxidising agents such as H_2O_2, O_3 and semiconductors such as TiO_2 and ZrO_2 associated with UV radiation, sound radiation and transition metals [20,21]. The oxidising agent absorbs energy from light decomposing in free radicals through diverse mechanisms [22]. Nevertheless, the association of oxidising species can promote a synergistic effect speeding up the generation of radicals [23].

Many studies have suggested that AOPs can enhance the toxicity of treated effluents due to the generation of more harmful intermediate species, characterising the treatment as ineffective [24,25]. Ecotoxicity tests represent an alternative tool to evaluate the potential risks associated with free radicals and partially oxidised species generated along the process [24,26], relating the side effects of the development of the organisms with the presence of harmful species [27]. Phytotoxicity is the study of the potential inhibition of chemical pollutants on seeds germination and plants growth [28]. *Lactuca sativa* L. (lettuce) is among the most used vegetables in phytotoxicity assays with a good reproducibility and low-cost resource [29].

Oxidising photochemical processes involve a complexity of reactions that is often difficult to be described by simple linear correlations, requiring more sophisticated techniques to achieve fitter kinetic models. Artificial neural networks (ANNs) are computer-based systems able to learn from the set of data and map input–output relationship. Recently, they have been increasingly applied to simulate kinetics of complex AOP systems in water treatment and even in decolourisation of samples [30–32], as ANNs do not require the physical and mathematical description of the phenomena involved in the process, solving the proposed problems by machine learning techniques [33]. They are pointed out as a great solution for complex non-linear problems which involve several inputs, helping to understand the interaction among the parameters and providing models where ANNs are able to predict effectively the statistical and mathematical behaviour of the systems.

In this study, UV-solar and UV-C based AOP systems were tested in the degradation of TT and BB samples. A factorial planning was performed in order to improve degradation time in the best of the AOP systems studied. Statistical studies were also carried out to study the influence of the variables in the process. A kinetic study was conducted with regression analysis of the data and compared with a mechanistic model developed for the process. Additionally, an ANN model was generated to describe the dyes degradation since it adjusts

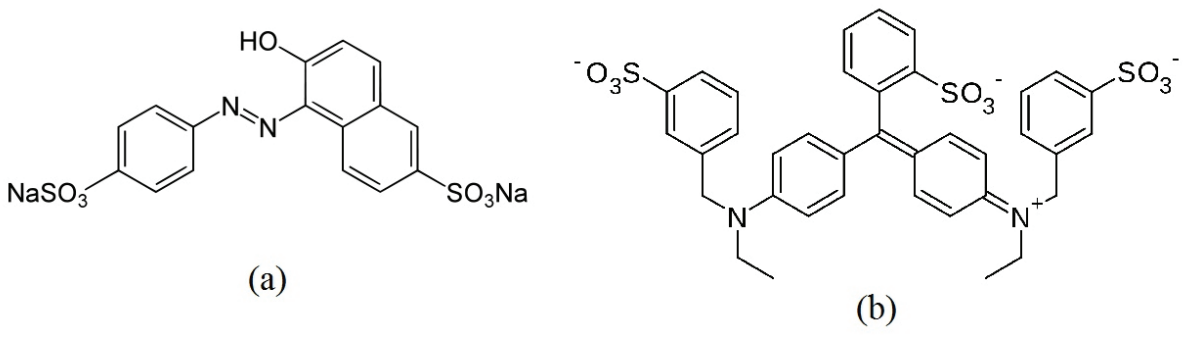

Fig. 1. Molecular structure of Tartrazine (a) and Brilliant Blue (b).

itself to face several variations on the response, maintaining precision as much as possible. Environmental quality parameters and phytotoxicity bioassays were analysed in order to guarantee the treatment efficiency.

2. Materials and methods

The treatment of the samples was conducted in 300 mL cylindrical glass recipients with 5.5 cm in height and 9.0 cm in diameter. The samples were prepared with 20 mg L^{-1} of TT and 20 mg L^{-1} of BB (F. Trajano Aromas e Ingredientes Ltda, Brazil) with distilled water. For each recipient, 250 mL of dyes solution was used. All the analyses were carried out in a UV–Vis spectrophotometer Spectroquant Pharo 300, and the absorbance peaks were read at wavelengths of 257, 411 and 627 nm for aromatics, TT and BB, respectively. Total degradation percentage of both dyes (%) was used as the response in the discussions.

During the treatments, the samples were subjected to magnetic stirring and carried out simultaneously to be collected alternately in order to not interfere in the system volumes. All the samples containing TiO_2 were decanted for 24 h in the dark and centrifuged at 3,500 rpm for 20 min before being analysed to ensure the absence of suspended TiO_2. Solar experiments were conducted at the same day time (9 am to 3 pm) and location (Recife, Brazil; 8°04′03″ S; 34°55′00″ W), during cloudless days to minimise variations in sunlight intensity. The temperature ranged from 30°C to 38°C in the solar treatments, measured after 30 min intervals until the end of the experiments. The UV-C light experiments were conducted in a bench photocatalytic reactor as shown in Fig. 2, preheated for 20 min to stabilise the UV-C emissions.

The reactors contained one germicide lamp (Ecolume 30W) and were internally coated with reflective material and supplied with air circulation to regulate internal temperature. Global light intensity was estimated to be about 6 W m^{-2}. The temperature of the samples was monitored during the treatments. In the solar radiation set of experiments, they ranged between 35.0°C and 41.3°C during the process. In the reactor set of experiments, the temperature ranged from 22.1°C to 26.7°C. According to Borges et al. [34], the continuous incidence of radiation can heat the system and disfavour radical global rates, reducing the rate-limiting step. The heat promoted in the reactor systems was not excessive due to outdoor room cooling.

Fig. 2. Bench photocatalytic reactor.

2.1. Preliminary tests

Preliminary tests were carried out during 360 min under solar radiation and a germicide lamp (UV-C radiation) in a photocatalytic reactor, analysing two variables: the presence of H_2O_2 and TiO_2, as shown in Table 1. The time set for the experiments was based on previous tests in similar systems. Experiments with no radiation source (dark chamber) and direct photolysis were also conducted as blanks to evaluate the influence of the radiation source and the presence of oxidant and photocatalyst in order to find the system with the best performance.

In all the experiments, 404 mg L^{-1} of AEROXIDE© TiO_2 P25 (Evonik Degussa Brasil Ltda, São Paulo, Brazil) in suspension and 9.2 mmol L^{-1} of H_2O_2 (Coremal | Pochteca©, Recife, Brazil) were used for 250 mL of the sample. TiO_2 amount was based on previous tests, while the H_2O_2 amount was calculated by the degradation reaction stoichiometry of the two dyes mixture (total 53 μL of H_2O_2 50% v/v) and it had the value duplicated. 53 μL were added at the beginning of the treatment and again 53 μL were added after 180 min in all cases. TiO_2 was applied as a catalyst and it was recovered at the end by centrifugation. The samples were collected after 1, 5, 10, 15, 20, 30, 60, 90, 120, 150, 180, 210, 240, 270, 300, 330 and 360 min.

2.2. Factorial experimental design to the UV-solar/H_2O_2/TiO_2 system

A 2^3 factorial planning was made for the best degradation performance system obtained in the preliminary tests. The studied parameters were H_2O_2, TiO_2 and time as shown in Table 2.

A complete factorial planning was carried out with 11 experiments. The central point (0, 0, 0) was run in triplicate to estimate the experimental error. The samples were collected before and after the treatments.

The statistical treatment of the data was run in Statistic Experimental Design 6.0 for the factorial planning experiments. The statistical significance of the variables from the

Table 1
AOP investigated systems for the preliminary tests

No radiation source	Solar radiation	UV-C radiation
H_2O_2	H_2O_2	H_2O_2
TiO_2	TiO_2	TiO_2
H_2O_2/TiO_2	H_2O_2/TiO_2	H_2O_2/TiO_2
–	Photolysis	Photolysis

Table 2
Variable codes for the 2^3 factorial planning

Code	H_2O_2 (mmol L^{-1})	TiO_2 (mg L^{-1})	Time (min)
–1	9.2	404	60
0	18.4	606	90
+1	27.6	808	120

factorial planning and a linear model was investigated, based on the variables adjusted to the experimental points. The response surface (RS) analysis was also conducted in order to verify the relation between the variables and the observed results. An empirical equation was obtained by the software.

2.3. Statistical and kinetic modelling study

2.3.1. Regression analysis of dyes degradation

The data of the best performance experiment from the factorial planning were adjusted to kinetic models of zero order, pseudo-first-order and pseudo-second-order through Microsoft Excel 2010© and a kinetic constant (Eq. (1)) and half-life time (Eq. (2)) were estimated for the best fitting the pseudo-first-order model.

$$\ln\left(\frac{[C_n)}{C_0}\right) = -kt \quad (1)$$

$$t_{1/2} = \ln 2/k \quad (2)$$

2.3.2. Mechanistic modelling of dyes degradation

A mechanistic model was developed for the reaction based on the known steps and the kinetic constants obtained, best fit on a pseudo-first-order model could be compared with the previous one obtained by regression analysis methodology.

2.3.3. Kinetic modelling using ANNs

The model used to describe the degradation behaviour of the best experiment obtained from the factorial planning was developed in Unity 3D©, using C# language. The method applied was a 1:4:1 network type (one input, four hidden layers and one output) in which the variable time of degradation was used as the input data. The training method is based on particle swarm optimization, where a small disturbance is induced in the weights and bias to verify if the resulting network fits well with the experimental data. All trainings were performed on a regular desktop computer.

2.4. Environmental quality parameters

The best degradation performance experiment obtained from the factorial planning was repeated under the same conditions in 10 vessels (2.5 L of dye solution). The samples were collected at intervals of 1, 5, 10, 15, 20, 30, 45, 60, 75, 90, 105, 120, 135 and 150 min.

Chemical oxygen demand (COD) and conductivity were determined for the samples before and after 120 min of treatment. The pH of the samples was also measured.

2.5. Acute phytotoxicity bioassay

Solutions of 100%, 75%, 50% and 25% (v/v) of the samples before and after the best performance treatment were prepared in quintuplicate with distilled water. 4 mL of each solution was used to wet filter papers containing 15 *Lactuca sativa* L. seeds in Petri plates. The plates were stored for 120 h at 22°C in a laboratory incubator. The positive control was carried out under the same conditions with distilled water and the negative control with mercurial sulphate (Hg_2SO_4) at 5 mmol L^{-1}. After incubation, the germinated seeds were quantified and length of their roots measured. Lethal concentration for 50% of the population (LC_{50}) was determined according to Dutka [35] and Greene et al. [36] methodologies.

3. Results and discussion

3.1. Preliminary tests

The experiments conducted in the absence of a radiation source did not reach significant degradation after 6 h in any of the systems studied as expected. Since there was no radiation source, the radicals could not be formed at significant rates and complex organic dyes, such as TT and BB, presented high resistance and stability [37].

3.1.1. UV-C experiments

The results for UV-C preliminary experiments are in Fig. 3.

Direct photolysis with UV-C radiation presented 14.13% and 1.45% of degradation for dyes and aromatics, respectively, after 360 min of treatment. UV-C/H_2O_2 system presented 99.96% for dyes degradation and 70.44% for aromatics after 360 min. UV-C/TiO_2 system exhibited 89.90% and 81.29% of dye and aromatics degradation each and UV-C/H_2O_2/TiO_2 system was the most efficient in the reactors providing 99.71% and 97.82% of degradation in 330 min for dyes and aromatics, respectively. The results for UV-C/H_2O_2 were not satisfactory for the aromatic compounds degradation and the UV-C/TiO_2 did not reach more than 90% of degradation after the proposed time for the tests.

3.1.2. UV-solar experiments

The results for the tests settled under solar radiation are presented in Fig. 4.

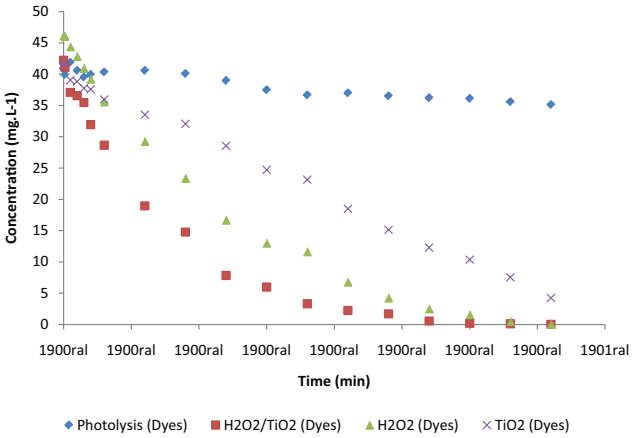

Fig. 3. Preliminary tests for the UV-C based experiments in the bench reactor.

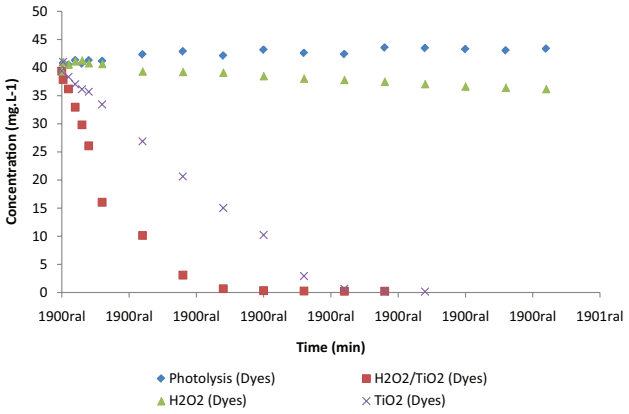

Fig. 4. Preliminary tests for the UV-solar based experiments.

No degradation was obtained with photolysis. According to Teixeira and Jardim [38], the photolysis process is expected to be less efficient in comparison with the other systems, as there is no generation of high oxidising radicals, taking the oxidising pathway of the targeted compounds much more energetic and less prone to occur. In addition, UV-solar/H_2O_2 system exhibited only 8.03% and 1.06% of dyes and aromatics degradation percentage after 360 min. This result, as expected, was less expressive than the UV-C system, because the solar light that reaches the Earth surface is composed mainly by UV-A (400–320 nm) and UV-B (320–280 nm), which has less energetic radiations than UV-C and H_2O_2 has an extension almost null in $\lambda > 290$ nm, 99% of solar radiation [39,40]. This subsequently explains the low efficiency of H_2O_2 in forming radical species under UV-solar radiation.

TiO_2 systems' performance under solar radiation presented better results than under UV-C radiation in general. The UV-solar/TiO_2 system exhibited a degradation percentage of 99.59% and 99.63% for dyes and aromatics, respectively, in 240 min while the UV-solar/TiO_2/H_2O_2 system reached 99.36% and 99.69% in only 180 min, half of the time proposed for the tests. The enhancement in degradation activity of UV-solar/TiO_2/H_2O_2 systems, when compared with UV-solar/TiO_2 is in accordance with previous reports in the literature. H_2O_2 has a synergistic effect in TiO_2 activity, improving the generation of radicals by absorbing UV-light in a wider wavelength range [41]. TiO_2 has a wider band gap energy extension, being photo-activated at $\lambda < 390$ nm [42], taking much more advantage of solar radiation than H_2O_2 alone being more efficient in the UV-A and UV-B range (UV-solar systems) than in the UV-C (reactor chamber systems).

Optimal results were expected for the reactor experiments due to UV-C radiation being more energetic than UV-solar radiation, however, the solar experiments are characterised by a higher spreading of light than in the designed reactor. In addition, the potency of the lamp is well-known for decreasing along with time and the reactor design is another point to be taken into consideration when explaining lower efficiency in UV-C experiments. After 360 min, the emissions were much weaker than in the beginning of the test, while solar emissions were continuous and less intermittent in a short time if not affected by external factors, despite being less energetic. Abeledo-Lameiro et al. [41] have also reported similar results which refer to the higher exposition surface for AOPs in outdoor experiments, providing higher efficiency of solar experiments when compared with germicide lamps.

The criteria for choosing the best performance system was reaching a high degradation percentage of compounds (>99%) in the shortest possible time. According to that criteria, UV-solar/H_2O_2/TiO_2 brought up the best results (99.36% of dyes degradation and 99.69% of aromatics in 180 min) and also represents a great cost of operation saving when compared with the UV-C/H_2O_2/TiO_2 (99.71% of dyes and 97.82% of aromatics in 330 min), since the radiation source is natural solar light. The limiting conditions of the chosen system are the dependence on the hour of the day and the weather, therefore, all of the experiments were carried out on sunny days.

3.2. Factorial experimental design to the UV-solar/H_2O_2/TiO_2 system

A 2^3 factorial planning was conducted for the best performance system, UV-solar/H_2O_2/TiO_2. Table 3 summarises the results of the factorial planning according to pre-established assays.

The largest degradation percentage was obtained in assay 8, when the greater amounts of H_2O_2 and TiO_2 were used, reaching high degradation percentage of dyes in 120 min.

The results for the degradation of assay 8 sampled at different times are exposed in Table 4.

As reported by the table, the system reached high degradation percentage after 90 min, by which time the samples were visually colourless. As expected, since there is a significant rate of radical generation due to the presence of TiO_2, the aromatics continued to be removed after the dyes have reached a high degradation percentage as it is observed due to the presence of remaining TiO_2 and radiation.

Table 3
Degradation results for the 2^3 factorial planning in the UV-solar/H_2O_2/TiO_2 system

Assay	H_2O_2 (μL)	TiO_2 (mg)	Time (min)	Aromatics degradation (%)	TT and BB degradation (%)
1	–	–	–	61.93	61.67
2	+	–	–	63.95	77.38
3	–	+	–	76.25	82.63
4	+	+	–	78.01	94.21
5	–	–	+	80.56	86.61
6	+	–	+	86.95	98.34
7	–	+	+	89.88	99.31
8	**+**	**+**	**+**	**96.70**	**99.80**
9	0	0	0	82.69	98.01
10	0	0	0	85.73	98.07
11	0	0	0	81.36	97.85

Note: Bold values represent the best results for the factorial planning experiment.

3.3. Statistical and kinetic modelling study

3.3.1. Empirical statistical model

An analysis of the variables significance is demonstrated in a Pareto chart (Fig. 5).

According to the chart, it is possible to conclude that all the variables have statistical significance when considering them both individually and the interactions among them. Time was the most significant variable followed by TiO_2 and H_2O_2 each individually.

Fig. 6 shows the RS analysis for the degradation of dyes combining the variables effect in pairs.

Table 4
Degradation results for the best result experiment from 2^3 factorial planning in the UV-solar/H_2O_2/TiO_2 system

Time (min)	Aromatics degradation (%)	TT and BB degradation (%)
1	5.74	5.35
5	17.10	26.54
10	28.53	35.65
15	41.18	49.40
20	52.54	61.61
30	61.43	77.14
45	71.04	90.84
60	80.20	95.25
75	85.65	98.35
90	**83.71**	**99.21**
105	92.83	99.26
120	95.31	99.37
135	98.33	99.37
150	99.89	99.57

Note: Bold values present the first result where colour was completely removed.

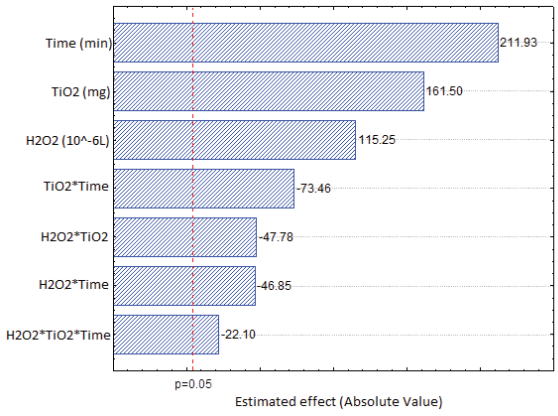

Fig. 5. Pareto chart of the 2^3 factorial planning experiments.

In all the charts, it is possible to observe the increase in variable amounts causing a subsequent increase in the degradation percentage of dyes, reflecting the statistical significance and assuring they were not in excess for the process. The excess of H_2O_2 could diminish the efficiency of the process by modifying selectivity and promoting undesired reactions [43]. It could also lead to quenching the hydroxyl radicals and the excess of TiO_2 in suspension could compromise the light harvesting and consequently, the global generation rate of radicals [44]. According to Figs. 5 and 6, time was the most significant variable in the process and it was not in excess since the degradation continues to be promoted over time as shown in the RS analysis.

From Statistic Experimental Design 6.0, a linear model was used to describe the degradation obtained in the experiment according to the statistical significance of the variables, as shown in Eq. (3).

$$D = 90.4842 + 8.5212X_{\text{time}} + 6.4938X_{\text{TiO}_2} + 4.6272X_{\text{H}_2\text{O}_2} - 2.9538X_{\text{TiO}_2}X_{\text{time}} - 1.9212X_{\text{H}_2\text{O}_2}X_{\text{TiO}_2} - 1.8838X_{H_2O_2}X_{\text{time}} - 0.8888X_{\text{H}_2\text{O}_2}X_{\text{TiO}_2}X_{\text{time}} \quad (3)$$

The chart for the residual analysis is represented in Fig. 7 by a red line along the experimental data obtained in the factorial planning. The residual model presented a reasonable adjustment for the experiment executed.

3.3.2. Regression analysis of dyes degradation

Regression analyses were conducted under the conditions of assay 8. The data were adjusted to kinetic models of zero-order, pseudo-first-order and pseudo-second-order through Microsoft Excel 2010© and the rate constants were estimated. The R^2 correlation coefficient used to opt for an adequate fitting model was more suitable for pseudo-first-order kinetics (R^2 = 0.943). In accordance with other reports, the kinetics of AOP degradation systems are more complex and could not be described by zero-order kinetic model due to dependence on different reaction steps, such as radical generation rates, radiant energy balance, mass transfer and distribution area of absorbed radiation [30,31]. Since the concentrations of radiation cannot be measured and considering (a) the reaction limiting step is the formation of radicals and (b) TiO_2 and H_2O_2 concentrations are in excess during most of the reaction time, the rate reaction follows the pseudo-first-order kinetics [45]. R^2 for zero-order and second-order models were 0.684 and 0.917, respectively. Fig. 8(a) displays the adjustment made with regression analysis for a pseudo-first-order model during the degradation experiment and Fig. 8(b) displays an adjustment reducing the time to satisfy condition (b).

It can be observed that the 90 min model provides a better fitting (R^2 = 0.998) for the kinetic model since the adjustment considers the time interval where H_2O_2 and TiO_2 could be considered in excess. The rate constant was estimated at k = 0.0541 min^{-1} and the half-life reaction time was $t_{1/2}$ = 12.81 min.

3.3.3. Mechanistic modelling of dyes degradation

The reactions based on AOP photo-oxidation pathways are exhibited in Eqs. (4)–(7) each of them with their respective rate constants (k_0, k_1, k_2 and k_3) are as follows:

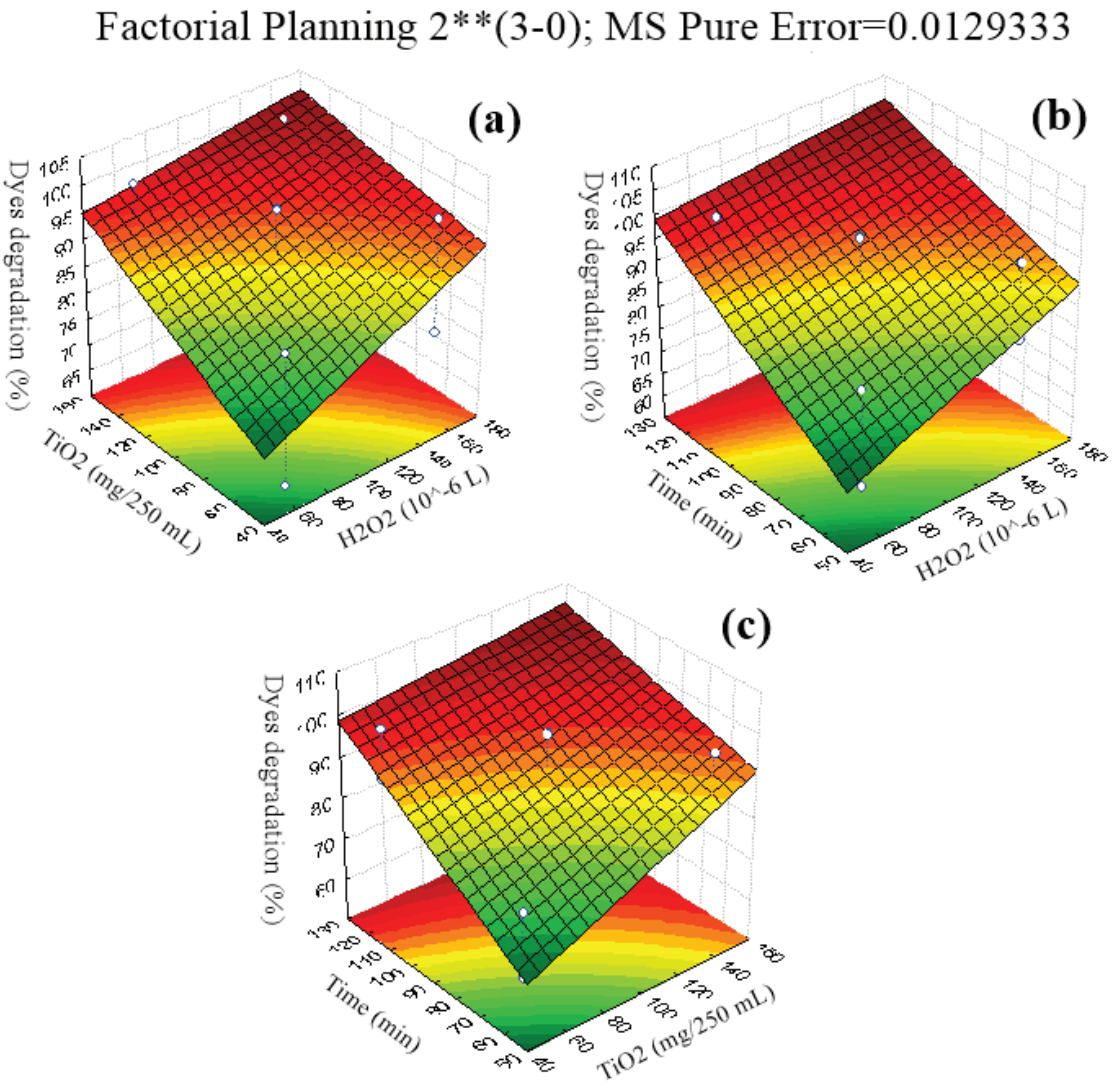

Fig. 6. Response surfaces for the degradation of dyes according to the variables TiO_2 and H_2O_2 (a), time and H_2O_2 (b) and time and TiO_2 (c).

$$H_2O_2 \xrightarrow{UV} 2^{\bullet}OH(k_0) \quad (4)$$

$$H_2O_2 + HO^{\bullet} \rightarrow H_2O^{\bullet} + H_2O(k_1) \quad (5)$$

$$^{\bullet}OH + \text{dyes} \rightarrow \text{degradation products } (k_2) \quad (6)$$

$$TiO_2 + \text{dyes}_{\text{adsorbed}} \xrightarrow{UV} \text{degradation products } (k_3) \quad (7)$$

Since the degradation of dyes is described by Eqs. (6) and (7), the following assumptions can be made:

$$\frac{dC}{dt} = -r_1 - r_2 \quad (8)$$

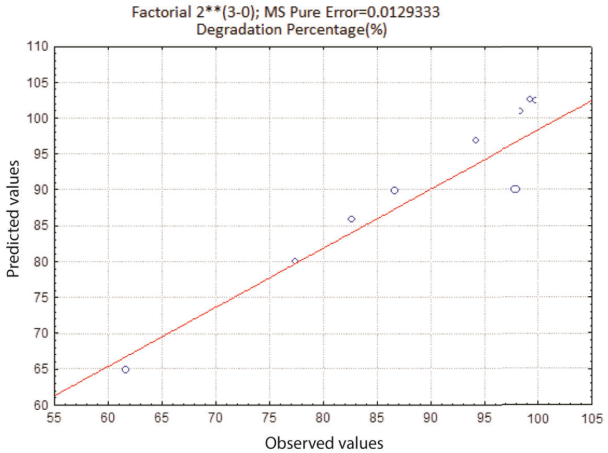

Fig. 7. Residual analysis obtained for TT and BB.

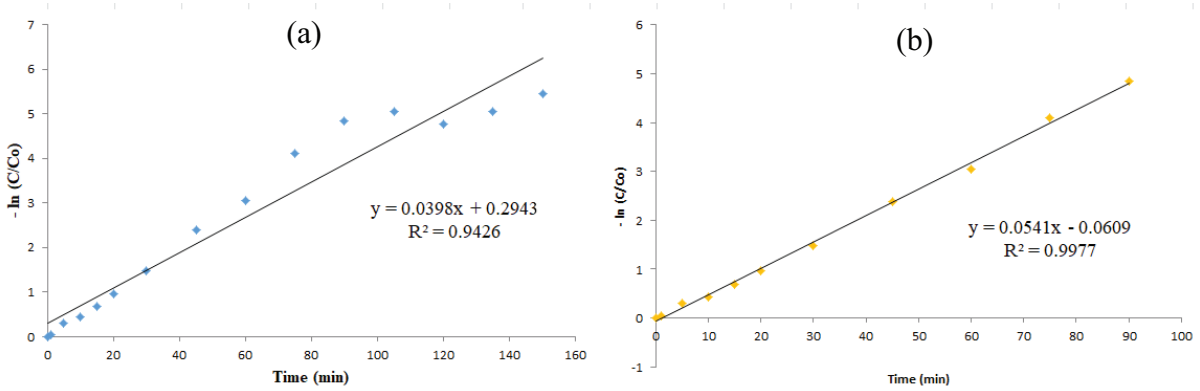

Fig. 8. Pseudo-first-order model for TT and BB degradation during the whole experiment (a) and adjusted to 90 min to improve the correlation with experimental data (b).

$$\frac{dC}{dt} = -k_1\left[{}^{\bullet}OH\right]\left[\text{dyes}\right] - k_2\left[\text{dyes}\right] \tag{9}$$

where [TiO_2] is 1 since it is in the solid state.

Thus, in order to get results one expression must be found for [•OH]:

$$\frac{d\left[{}^{\bullet}OH\right]}{dt} = -k_3\left[{}^{\bullet}OH\right]\left[H_2O_2\right] - k_0\left[H_2O_2\right] \tag{10}$$

Rearranging the differential equation, we obtain:

$$\frac{d\left[{}^{\bullet}OH\right]}{dt} + k_3\left[{}^{\bullet}OH\right]\left[H_2O_2\right] = -k_0\left[H_2O_2\right] \tag{11}$$

Since H_2O_2 is in excess over the time, then the coefficients of the differential equation are constants providing the solution:

$$y(x) = e^{-\int p(x)dx}\left(\int q(x)e^{\int p(x)dx}dx + C\right) \tag{12}$$

$$fp(x)dx = k_3\left[{}^{\bullet}OH\right]\left[H_2O_2\right] \tag{13}$$

$$\int\left(-k_0\left[H_2O_2\right]e^{k_3\left[{}^{\bullet}OH\right]\left[H_2O_2\right]}d\left[{}^{\bullet}OH\right] + C\right) = -\frac{k_0\left[H_2O_2\right]}{k_3\left[H_2O_2\right]}e^{k_3\left[{}^{\bullet}OH\right]\left[H_2O_2\right]} + C_0 \tag{14}$$

where C_0 is he initial value for [•OH]. Finally, it is obtained that:

$$\left[{}^{\bullet}OH\right] = e^{k_3\left[{}^{\bullet}OH\right]\left[H_2O_2\right]}\left(-\frac{k_0}{k_3}e^{k_3\left[{}^{\bullet}OH\right]\left[H_2O_2\right]} + C_0\right) \tag{15}$$

$$\left[{}^{\bullet}OH\right] = \left(-\frac{k_0}{k_3}\right) \tag{16}$$

Substituting in Eq. (9):

$$\frac{dC}{dt} = -k_1\left(-\frac{k_0}{k_3}\right)\left[\text{dyes}\right] - k_2\left[\text{dyes}\right] \tag{17}$$

Grouping the terms, we obtain a simple final expression for the AOP system dependant on each step of reaction.

$$\frac{dC}{dt} = \left(\frac{k_1k_0}{k_3} - k_2\right)\left[\text{dyes}\right] \tag{18}$$

As it can be observed by the mechanistic analysis, Eq. (18) describes a first-order reaction and the rate constants can be compared with regression analysis results. The application of this simple model was based on more complex principles, corroborates with the kinetic principles known for AOP.

$$\left(\frac{k_1k_0}{k_3} - k_2\right) = k = 0.0398\,\text{min}^{-1} \tag{19}$$

where k represents the global rate constant.

The model did not present a considerable fitting for the experimental data with a relative error of 26.4% compared with the value obtained in the regression analysis. As stated by Teixeira and Jardim [38], the degradation of large organic molecules with different functional groups in AOPs systems can be more commonly associated with pseudo-first-order models. Bibak and Aliaabadi [46] studied the removal of Malachite Green by photolysis and photocatalysis with TiO_2 and the experiments were better adjusted for pseudo-first-order kinetics as well as Vianna and Tôrres [47], which also points the degradation of other synthetic food dyes to be of pseudo-first-order kinetics by photo-oxidation methods. Since the adjustment does not present very accurate results for a large range of the experiments, ANNs were used in order to achieve an optimised adjustment.

3.3.4. Kinetic modelling using ANNs

To guarantee the reliability and fastness of the ANN analysis, the core and the axon values were normalised and the

input and output adjusted between –1 and 1 for all set of data. The characteristics of the training for input and output data are described in Table 5. [C/C_0] represents the decolourisation efficiency as the result of the training when the time is varied.

Several topologies were tested and the training took around 3 h to be finished. The optimised result was defined by the lower mean absolute error obtained for UV-solar/TiO_2/H_2O_2. The ANN model for the degradation data of dyes is in Fig. 9.

It is possible to observe the input (time of degradation), the weight values (above the connection lines between the neurons) and the bias (the arrows pointing to the neurons). The weight represents the values which multiply the output values of a neuron before the value gets to the next neuron and the bias, the values added to the neuron inputs. The lower mean absolute error obtained by the data were 0.013554697. This model is able to predict the degradation response for the solar AOP process under the given conditions.

Fig. 10 shows the training result for the dyes degradation in comparison with the experimental data.

It is possible to observe that the adjustment was reached with low absolute mean error representing accurately the experiment. A good generalisation could be achieved by the training to predict the removal of TT and BB and more than 121,000 interactions were necessary. The ANN model can detect subtle change on experimental conditions since all the experimental points fit considerably with the network. Then, the model generalises the set of data well.

Table 5
Range of input and output parameters

Variable	Range
Input layer	
Time (min)	0–150
[C_0] (mg L^{-1})	39.41
Output layer	
[C/C_0] (mg L^{-1})	–0.0114 to 0.9691

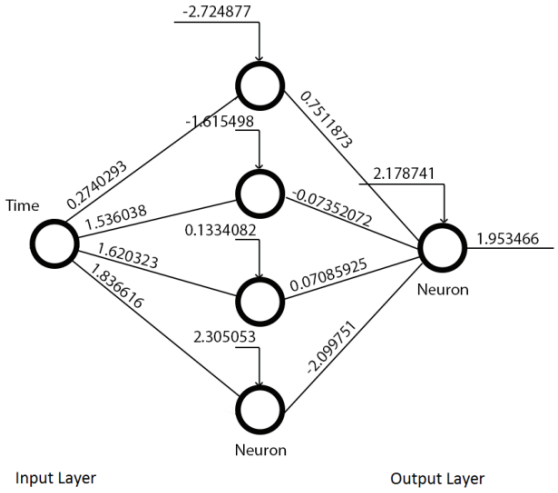

Fig. 9. Artificial neural network model for TT and BB degradation.

3.4. Environmental quality parameters

Additional analyses to enforce the purposes of the treatment were carried out to investigate the by-products of the AOP system. Table 6 shows the results of environmental quality parameters tested.

COD, which represents the total organic matter degraded by a chemical oxidant, is reduced by at least 91.35% from the raw sample indicating an improvement in water quality since the number of oxidisable pollutants is reduced. The COD of the sample after the treatment could not be quantified due to the detection limit of the analysis method (10.00 mg L^{-1} minimum). AOPs reaction pathway leads to the formation of ionic species from the functional groups of organic molecules [20] such as sulphate ion and nitrogen oxides. The conductivity analysis confirms the generation of ionic species after the degradation, exhibiting an approximate four times rise in sample conductivity. The pH of the sample before the treatment was estimated at 6.34 and after the treatment at 6.12. The smooth reduction in the pH after the treatment can be explained by the generation of ionic species and CO_2 during the radicals attack to organic molecules of dyes [20,21].

3.5. Acute phytotoxicity bioassay

The LC_{50} was calculated from the assay with samples before and after the treatment and *Q* tests were applied to statistical outliers in data. The stalk percentage growth of the *Lactuca sativa* in the samples was compared with the growth obtained in the positive control with distilled water. LC_{50} values

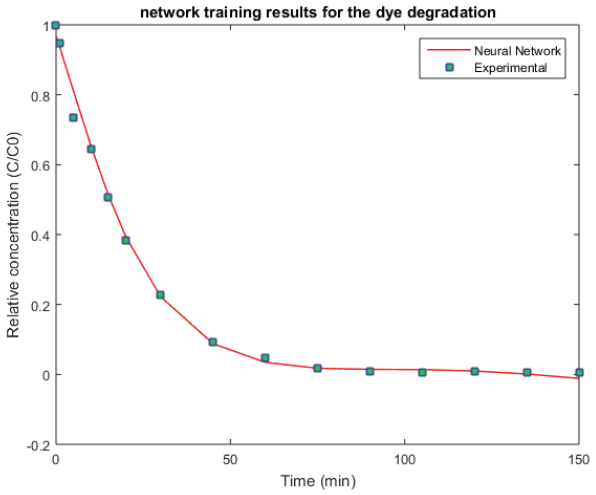

Fig. 10. Resulting neural network training for TT and BB degradation.

Table 6
Analysis of the environmental quality parameters for the samples before and after the treatment

Sample	COD (mg L^{-1})	Conductivity (μS cm^{-1})	pH
Before AOP	115.6	20.71	6.34
After AOP	BDL[a]	85.50	6.12

[a]BDL, below detection limits (~10 mg L^{-1}).

obtained were 39.31% ± 2.57% and 87.73% ± 7.95% for the non-treated and treated samples, respectively. These results indicate a concentration of 39.31% (v/v) of the non-treated sample to inhibit 50% of stalk growth would be required, while 87.73% (v/v) of treated sample would cause the same effect. The treatment is efficient not only to degrade the compounds but also to reduce acute phytotoxicity of water solutions and more phytotoxic by-products were not formed.

4. Conclusions

It was possible to study different systems and set the best performance system among them for the removal of TT and BB samples and note the synergistic effect of H_2O_2 and TiO_2 association. UV-solar/H_2O_2/TiO_2 system also represents a minimisation of costs and a cleaner alternative to effluent treatment. The factorial planning could enhance the performance of the experiments shortening the total time under different amounts. An appropriate adjustment could be made by ANN modelling to predict the degradation of the system under fixed conditions along with time. The phytotoxicity tests assured the efficiency of the treatment in reducing the toxic potential of the sample, enhancing the LC_{50} for the treated samples in comparison with the raw solution and further analyses corroborate the improvement in the sample water quality. From these results, the UV-solar/H_2O_2/TiO_2 system is proved to be a suitable tool in the removal of TT and BB from aqueous solutions.

References

[1] J. Jiao, J. Wang, M. Li, J. Li, Q. Li, Q. Quan, J. Chen, Simultaneous determination of three azo dyes in food product by ion mobility spectrometry, J. Chromatogr., B, 1205 (2016) 105–109.

[2] R. Shiralipour, A. Larki, Pre-concentration and determination of tartrazine dye from aqueous solutions using modified cellulose nanosponges, Ecotoxicol. Environ. Saf., 135 (2017) 123–129.

[3] C. Tsai, C. Kuo, D.Y. Shih, Determination of 20 synthetic dyes in chili powders and syrup-preserved fruits by liquid chromatography/tandem mass spectrometry, J. Food Drug Anal., 23 (2015) 453–462.

[4] G.L. Dotto, E.C. Lima, L.A.A. Pinto, Biosorption of food dyes onto *Spirulina platensis* nanoparticles: equilibrium isotherm and thermodynamic analysis, Bioresour. Technol. 103 (2012) 123–130.

[5] S.K. Sen, S. Raut, P. Bandyopadhyay, S. Raut, Fungal decolouration and degradation of azo dyes: a review, Fungal Biol. Rev., 30 (2016) 112–133.

[6] L. Ji, Q. Cheng, K. Wu, X. Yang, Cu-BTC frameworks-based electrochemical sensing platform for rapid and simple determination of Sunset yellow and tartrazine, Sens. Actuators, B, 231 (2016) 12–17.

[7] K. Yamjala, M.S. Kainar, N.R. Ramisetti, Methods for the analysis of azo dyes employed in food industry – a review, Food Chem., 192 (2016) 813–824.

[8] H. Sun, F. Wang, L. Ai, Determination of banned 10 azo-dyes in hot chili products by gel permeation chromatography–liquid chromatography-electrospray ionization-tandem mass spectrometry, J. Chromatogr., A, 1164 (2007) 120–128.

[9] M.J. Scotter, Overview of EU Regulation and Safety Assessment for Food Colours, Chapter 3, Colour Additives for Foods and Beverages, Woodhead Publishing, Kidlington (OX), 2015, pp. 61–74.

[10] M.O. Dawodu, K.G. Akpomie, Evaluating the potential of a Nigerian soil as an adsorbent for tartrazine dye: isotherm, kinetic and thermodynamic studies, Alexandria Eng. J., 55 (2016) 3211–3218.

[11] J. Goscianska, R. Pietrzak, Removal of tartrazine from aqueous solution by carbon nanotubes decorated with silver nanoparticles, Catal. Today, 249 (2015) 259–264.

[12] A. Mohamed, A. Galal, Y. Elewa, Comparative protective effects of royal jelly and cod liver oil against neurotoxic impact of tartrazine on male rat pups brain, Acta Histochrm., 117 (2015) 649–658.

[13] X. Qiu, L. Lu, J. Leng, Y. Yu, W. Wang, M. Jiang, L. Bai, An enhanced electrochemical platform based on graphene oxide and multi-walled carbon nanotubes nanocomposite for sensitive determination of Sunset Yellow and tartrazine, Food Chem., 190 (2016) 889–895.

[14] C. Morris, S.J. Mooney, S.D. Young, Sorption and desorption characteristics of the dye tracer, Brilliant Blue FCF, in sandy and clay soils, Geoderma, 146 (2008) 434–438.

[15] Y. Chen, C. Tsen, S. How, C. Lo, W. Chou, S. Wang, Amyloid fibrillogenesis of lysozyme is suppressed by a food additive brilliant blue FCF, Colloids Surf., B, 142 (2016) 351–359.

[16] V.K. Gupta, A. Mitall, L. Krishnan, J. Mittal, Adsorption treatment and recovery of the hazardous dye, Brilliant Blue FCF, over bottom ash and de-oiled soya, J. Colloid Interface Sci., 293 (2006) 16–26.

[17] S. Antakli, L. Nejen, S. Katran, Simultaneous determination of tartrazine and brilliant blue in foodstuffs by spectrophotometric method, Int. J. Pharm. Pharm. Sci., 7 (2015) 214–218.

[18] Z. Shu, H. Wu, H. Lin, T. Li, Y. Liu, F. Ye, X. Mu, X. Li, X. Jiang, J. Huang, Decolourization of Remazol Brilliant Blue R using a novel acyltransferase-ISCO (in situ chemical oxidation) coupled system, Biochem. Eng. J., 115 (2016) 56–63.

[19] R.K. Gautam, P.K. Gautam, S. Banerjee, V. Rawat, S. Soni, S.K. Sharma, M.C. Chattopadhyaya, Removal of tartrazine by activated carbon biosorbents of *Lantana camara*: kinetics, equilibrium modeling and spectroscopic analysis, J. Environ. Chem. Eng., 3 (2015) 79–88.

[20] O. Rozas, C. Vidal, C. Baeza, W.F. Jardim, A. Rossner, H.D. Mansilla, Organic micropollutants (OMPs) in natural waters: oxidation by UV/H_2O_2 treatment and toxicity assessment, Water Res., 98 (2016) 109–118.

[21] M.P. Rayaroth, U.K. Aravind, C.T. Aravindakumar, Sonochemical degradation of Coomassie Brilliant Blue: effect of frequency, power density, pH and various additives, Chemosphere, 119 (2015) 848–855.

[22] A. Adak, K.P. Mangalgiri, J. Lee, L. Blaney, UV irradiation and UV-H_2O_2 advanced oxidation of the roxarsone and nitarsone organoarsenicals, Water Res., 70 (2015) 74–85.

[23] P. Raiazada, P. Shandilya, P. Singh, P. Thakur, Solar light-facilitated oxytetracycline removal from the aqueous phase utilizing a H_2O_2/$ZnWO_4$/CaO catalytic system, J. Taibah Univ. Sci., 11 (2016) 689–699.

[24] M. Brienza, M.M. Ahmed, A. Escande, G. Plantard, L. Scrano, S. Chiron, S.A. Bufo, V. Goetz, Use of solar advanced oxidation processes for wastewater treatment: follow-up on degradation products, acute toxicity, genotoxicity and estrogenicity, Chemosphere, 148 (2016) 473–480.

[25] H. Gong, W. Chu, Determination and toxicity evaluation of the generated products in sulfamethoxazole degradation by UV/$CoFe_2O_4$/TiO_2, J. Hazard. Mater., 314 (2016) 197–203.

[26] D. Rede, L.H. Santos, S. Ramos, F. Oliva-Teles, C. Antao, S.R. Sousa, C. Delerue-Matos, Ecotoxicological impact of two soil remediation treatments in *Lactuca sativa* seeds, Chemosphere, 159 (2016) 193–198.

[27] Q. Zhang, F. Wang, C. Xue, C. Wang, S. Chi, J. Zhang, Comparative toxicity of nonylphenol, nonylphenol-4-ethoxylate and nonylphenol-10-ethoxylate to wheat seedlings (*Triticum aestivum* L.), Ecotoxicol. Environ. Saf., 131 (2016) 7–13.

[28] W. Shen, N. Zhu, J. Cui, H. Wang, Z. Dang, P. Wu, Y. Luo, C. Shi, Ecotoxicity monitoring and bioindicator screening of oil-contaminated soil during bioremediation, Ecotoxicol. Environ. Saf., 124 (2016) 120–128.

[29] L.C. Rodrigues, S. Barbosa, M. Pazin, B.S. Maselli, L.A. Beijo, F. Kummrow, Phytotoxicity and cytogenotoxicity of water and urban stream sediment in bioassay with *Lactuca sativa,* Rev. Bras. Eng. Agríc. Ambient., 17 (2013) 1099–1108.

[30] A.R. Khataee, O. Mirzajani, UV/peroxydisulfate oxidation of C. I. Basic Blue 3: modeling of key factors by artificial neural network, Desalination, 251 (2010) 64–69.
[31] A.R. Soleymani, J. Saien, H. Bayat, Artificial neural networks developed for prediction of dye decolorization efficiency with UV/$K_2S_2O_8$ process, Chem. Eng. J., 170 (2011) 29–35.
[32] N. Dhiman, Markandeya, A. Singh, N.K. Verma, N. Ajaria, S. Patnaik, Statistical optimization and artificial neural network modeling for acridine orange dye degradation using in-situ synthesized polymer capped ZnO nanoparticles, J. Colloid Interface Sci., 493 (2017) 295–306.
[33] S. Haykin, Redes neurais, princípios e prática, Artmed, São Paulo, 2001, pp. 28–45.
[34] M.E. Borges, M. Sierra, E. Cuevas, R.D. García, P. Esparza, Photocatalysis with solar energy: sunlight-responsive photocatalyst based on TiO_2 loaded on a natural material for wastewater treatment, Sol. Energy, 135 (2016) 527–535.
[35] B. Dutka, Short-Term Root Elongation Toxicity Bioassay: Methods for Toxicological Analysis of Waters, Wastewaters and Sediments, National Water Research Institute (NWRI), Burlington, ON, 1989.
[36] J.C. Greene, C.L. Bartels, W.J. Warren-Hicks, B.R. Parkhurst, G. Linder, S.A. Peterson, W.E. Miller, Protocols for Short-Term Toxicity Screening of Hazardous Waste Sites, U.S. EPA 600/3-88/029, Corvallis, OR, 1988.
[37] R. Giovannetti, C.A.D. Amato, M. Zannotti, E. Rommozzi, R. Gunnella, M. Minicucci, A. Di Cicco, Visible light photoactivity of polypropylene coated nano-TiO_2 for dyes degradation in water, Sci. Rep., 5 (2015) 17801–17813.
[38] C.P. Teixeira, W.F. Jardim, Advanced Oxidative Processes: Theoretical Foundations, Caderno Temático, Campinas, SP, Brazilian, 2004.
[39] C. Lin, H. Lin, L. Hsu, Degradation of ofloxacin using UV/H_2O_2 process in a large photoreactor, Sep. Purif. Technol., 168 (2016) 57–61.
[40] D. Rubio, E. Nebot, J.F. Casanueva, C. Pulgarin, Comparative effect of simulated solar light, UV, UV/H_2O_2 and photo-Fenton treatment (UV–Vis/H_2O_2/$Fe^{2+,3+}$) in the *Escherichia coli* inactivation in artificial seawater, Water Res., 47 (2013) 6367–6379.
[41] M.J. Abeledo-Lameiro, A. Reboredo-Fernández, M.I. Polo-López, P.F. Fernández-Ibâñez, E. Ares-Mazás, H. Gómez-Couso, Photocatalytic inactivation of the waterborne protozoan parasite *Cryptosporidium parvum* using TiO_2/H_2O_2 under simulated and natural solar conditions, Catal. Today, 280 (2017) 132–138.
[42] S. Li, R.J. Erickson, L.K. Wallis, S.A. Diamond, D.J. Hoff, Modelling TiO_2 nanoparticle phototoxicity: the importance of chemical concentration, ultraviolet radiation intensity, and time, Environ. Pollut., 205 (2015) 327–332.
[43] G. Gallina, P. Biasi, J. García-Serna, T. Salmi, J. Mikkola, Optimized H_2O_2 production in a trickled bed reactor, using water and methanol enriched with selectivity promoters, Chem. Eng. Sci., 123 (2015) 334–340.
[44] R.K. Chava, W. Lee, S. Oh, K. Jeong, Y. Yu, Improvement in light harvesting and device performance of dye sensitized solar cells using electrophoretic deposited hollow TiO_2 NPs scattering layer, Sol. Energy Mater. Sol. Cells, 161 (2017) 255–262.
[45] D. Fabbri, M. Minella, V. Maurino, C. Minero, D. Vione, A model assessment of the importance of direct photolysis in the photo-fate of cephalosporins in surface waters: possible formation of toxic intermediates, Chemosphere, 134 (2015) 452–458.
[46] O. Bibak, M. Aliaabadi, Photocatalytic degradation of malachite green in aqueous solution using TiO_2 nanocatalyst, J. Biodivers. Environ. Sci., 5 (2014) 301–310.
[47] V.B. Vianna, A.R. Tôrres, Degradation of acid dyes for advanced oxidation processes with a low-speed round disc reactor, Quim. Nova, 31 (2008) 1353–1358.